

Published in final edited form as:

Biochemistry. 2013 November 19; 52(46): . doi:10.1021/bi401116n.

Metabolic Flux Between Unsaturated and Saturated Fatty Acids is Controlled by the FabA:FabB Ratio in the Fully Reconstituted Fatty Acid Biosynthetic Pathway of *E. coli*[#]

Xirui Xiao^a, Xingye Yu^b, and Chaitan Khosla^{a,b,*}

^aDepartment of Chemistry, Stanford University, Stanford CA 94305

^bDepartment of Chemical Engineering, Stanford University, Stanford CA 94305

Abstract

The entire fatty acid biosynthetic pathway from *Escherichia coli*, starting from the acetyl-CoA carboxylase, has been reconstituted *in vitro* from fourteen purified protein components. Radiotracer analysis verified stoichiometric conversion of acetyl-CoA and NAD(P)H into the free fatty acid product, allowing implementation of a facile spectrophotometric assay for kinetic analysis of this multi-enzyme system. At steady state, a maximum turnover rate of 0.5 s⁻¹ was achieved. Under optimal turnover conditions, the predominant products were C₁₆ and C₁₈ saturated as well as monounsaturated fatty acids. The reconstituted system allowed us to quantitatively interrogate the factors that influence metabolic flux toward unsaturated versus saturated fatty acids. In particular, the concentrations of the dehydratase FabA and the β-ketoacyl synthase FabB were found to be crucial for controlling this property. By altering these variables, the percentage of unsaturated fatty acid produced could be adjusted between 10 and 50% without significantly affecting the maximum turnover rate of the pathway. Our reconstituted system provides a powerful tool to understand and engineer rate-limiting and regulatory steps in this complex and practically significant metabolic pathway.

The fatty acid biosynthetic pathway of *Escherichia coli* produces a range of fatty acids with varying chain lengths and degrees of unsaturation.¹ In addition to being of central importance in cell physiology,^{2, 3} this chemical variability also has industrial relevance. For example, the fraction of unsaturated fatty acids in microbial biodiesel influences its cetane number, cloud point, and stability.⁴⁻⁶

In an effort to quantitatively understand the factors that influence the productivity and product profile of this metabolic pathway, we recently reconstituted from purified protein components the *E. coli* fatty acid synthase comprised of nine subunits (FabA, FabB, FabD, FabF, FabG, FabH, FabI, FabZ, and the acyl carrier protein (ACP)) and a terminal thioesterase (TesA) responsible for chain release (Figure 1).⁷ Whereas ACP-bound fatty acyl chains are directly channeled into lipid biosynthesis *in vivo*, TesA was added to our reconstituted system to facilitate turnover. Here we have extended our *in vitro* system by including the four-subunit acetyl-CoA carboxylase (comprised of AccA, AccB, AccC, and AccD) (Figure 1). We have also developed spectrophotometric, GC-MS and GC-FID assays

[#]Research in this report was funded by LS9, Inc., and by a grant from the National Institutes of Health (GM 087934)

^{*}To whom correspondence should be addressed. Contact information: Prof. Chaitan Khosla, Address: Department of Chemistry, Stanford University, Stanford CA 94305, Telephone: 650-7236538, Fax number: 650-7250259, khosla@stanford.edu.

Supporting Information available

Supporting information includes details about plasmid construction, pI values of proteins. This material is available free of charge via the internet at <http://pubs.acs.org>.

for facile quantitative analysis of the entire biosynthetic pathway. In addition to establishing the requirements for maximum turnover of this complex multi-enzyme system, our studies have highlighted how metabolic flux is controlled to modulate the ratio of saturated and unsaturated products.

Experimental Procedures

Plasmid construction

Genes encoding AccA and AccC were amplified by PCR (Table S1) from *E. coli* BL21(DE3) genomic DNA using the DNeasy Blood and Tissue Kit (Qiagen) and inserted into pET28 via NdeI and EcoRI sites (for *accA*) or NdeI and XhoI sites (for *accC*). The resulting plasmids, pXY30 (carrying *accA*) and pXY42 (carrying *accC*), were used for the production of corresponding proteins (Table S2). Genes encoding AccB and AccD were synthesized by DNA2.0 (Menlo Park, CA) and placed into pJexpress411 (<https://www.dna20.com/pJexpress.php>). One of the two resulting plasmids, pJexpress411-AccD was used directly for AccD expression and purification. The *apo*-AccB expression plasmid, pXY31, was constructed by isolating the corresponding gene from pJexpress411-AccB and inserting it between the NdeI and EcoRI sites of pET28.

Protein purification

Components of the fatty acid synthase (FabA, FabB, FabD, FabF, FabG, FabH, FabI, FabZ, and *holo*-ACP) and the thioesterase (TesA) were purified as previously reported.³ Components of the acetyl-CoA carboxylase were purified similarly. For the purification of AccA, AccC, and AccD, an *E. coli* BL21(DE3) strain harboring the appropriate plasmid (pXY30, pXY42, or pJexpress411-AccD, respectively) was grown in LB-Miller broth supplemented with 50 µg/mL kanamycin at 37°C. The culture was cooled to 18°C at an OD₆₀₀ of 0.6. At that point protein expression was induced by adding 100 µM IPTG, and growth was continued for 16–20 h. To obtain pure *holo*-AccB, *E. coli* BL21(DE3) was co-transformed with two plasmids, pXY31 and pCY216.⁸ The culture medium contained 34 µg/mL chloramphenicol in addition to 50 µg/mL kanamycin, and 15 µM biotin and 500 µM IPTG were added at the point of induction. Cells were collected by centrifugation and lysed by sonication. The lysate was centrifuged, and the supernatant was applied to a Ni-NTA column (Qiagen) followed by further purification on a HiTrap Q anion exchange column (GE Healthcare). On a 0–1 M NaCl gradient, AccA, *holo*-AccB, AccC, and AccD eluted at approximately 150, 100, 250, and 200 mM NaCl, respectively. Buffer pH values were 1 unit higher than the calculated pI of the particular protein (see Table S3 for details). For AccB purification, an additional monomeric avidin column (Promega) was used to obtain highly pure biotinylated AccB (*holo*-AccB). The degree of biotinylation was verified by MALDI-TOF. Due to proteolytic susceptibility of AccC, Complete Protease Inhibitor (Roche) was added to the lysis buffer before sonication (1 tablet/30 mL resuspended cells in lysis buffer). All purified proteins were flash-frozen and stored in aliquots at –80°C.

Although earlier researchers^{9, 10} have reported aggregation of AccB during purification, our protein preparation did not appear to suffer from this problem. Whereas the precise reason for this difference remains unknown, it should be noted that earlier methods involved purification of AccB-AccC complexes, followed by separation of AccB via relatively harsh preparative methods. In contrast we have been able to express and purify *holo*-AccB as a stand-alone protein in its native form.

Kinetic assays

Radioactive assays were performed as previously described.⁷ For UV spectrophotometric assays, protein components of a reaction were thoroughly mixed (by gentle tapping for 10 s)

in 100 mM sodium phosphate buffer (pH 7.5) containing 1 mM TCEP. Another cocktail mixture of substrates and cofactors, including acetyl-CoA, NADPH, ATP and MgCl₂, was prepared separately in 200 μL tubes and stored on ice. Reactions were initiated by the addition of sodium bicarbonate. All reactions had a minimal volume of 60 μL. Upon initiation, the contents were quickly mixed and immediately transferred to a UV cuvette (Eppendorf). Absorbance at 340 nm was measured as a function of time in a LAMBDA 25 UV-VIS spectrophotometer (Perkin Elmer) using a path length of 0.2 cm.

Product analysis

Assay mixtures, prepared as described above, were incubated at room temperature for 16–18 h. Thereafter, 5% (v/v) acetic acid was added to quench the reaction. A total amount of 20 nmol pentadecenoic acid (MP Bio) was added as an internal standard. The mixture was then extracted twice with equal volume of ethyl acetate. The organic layer was dried in a Speedvac at room temperature, and re-dissolved in 20 – 25 μL butyl acetate. The resulting solution was subjected to derivatization with 20 μL N,O-Bis(trimethylsilyl)trifluoroacetamide (BSTFA) (Fluka) to form fatty silyl esters.

GC-MS analysis was employed to establish the identities of different species of fatty acid products in a reaction mixture. Experiments were performed on a 6850 Series II Network GC System coupled with 5975B VL Mass Selective Detector (Agilent). The GC column used was DB1-HT (J&W). A split injection mode (20:1) was used with the following GC temperature gradient: injection temperature 320 °C, initial column temperature 60 °C, initial hold time 3 min, program rate 20 °C/min, final column temperature 320 °C, final hold time 5 min. The total GC-MS run time was 20 min.

GC-FID analyses were employed for quantitative analysis of the relative abundance of individual fatty acid species in reaction mixtures. Analyses were performed on a 6890N GC system coupled with flame ionization detector (Agilent). A J&W Scientific DB-1 column was used with nitrogen as the carrier gas. A split injection mode (50:1) was used with the following GC temperature gradient: injection temperature 320 °C, initial column temperature 60 °C, initial hold time 1min, program rate 25 °C/min, final column temperature 300 °C, final hold time 0.9 min. The total GC-FID run time was 10 min.

Aqueous calibration standards were made of saturated fatty acid lauric acid, tetradecanoic acid, tetradecanoic acid, hexadecanoic acid, octadecanoic acid (all from Sigma-Aldrich), and mono unsaturated acids *cis*-5-dodecenoic acid, *cis*-9-tetradecenoic acid, *cis*-9-hexadecenoic acid, *cis*-11-octadecenoic acid (all from Nu-Check). We used *cis*-9-tetradecenoic acid as an analog for quantification due to the unavailability of *cis*-7-tetradecenoic acid, the actual product in our system. Authentic standards were prepared in the range of 20–1000 mg/L, and derivatized with BSTFA immediately before analysis. Identities of unsaturated fatty acids were confirmed by comparing retention times with authentic standards.

Results

Spectrophotometric analysis of the fatty acid synthase

We previously reported reconstitution of the *E. coli* fatty acid synthase using purified subunits plus TesA as a catalyst for the release of free fatty acid products via acyl-ACP hydrolysis.⁷ In that study reaction rates were radioisotopically measured using ¹⁴C-malonyl-CoA as the radiolabeled substrate, followed by product quantification via radio-TLC. Although this procedure allowed direct visualization of products, it required expensive, radioactive reagents and was labor intensive. Because stoichiometric conversion of the radiolabeled substrate into product was observed, we sought to develop a

spectrophotometric assay in which the rate of fatty acid production was derived from the rate of decrease in A_{340} due to NADPH oxidation.

To verify the stoichiometric conversion of NADPH into fatty acids under our assay conditions, the inability of the protein mixture to oxidize NADPH in the absence of other substrates was first confirmed (data not shown). Next, it was shown that the initial rate measurements by the two protocols were comparable under two representative assay conditions (Figure 2A and B, Table 1). An advantage of the spectrophotometric assay was its ability to monitor the initial stages of the assay under fast turnover conditions (see, for example, Figure 2B).

In vitro* reconstitution and kinetic analysis of the complete fatty acid biosynthetic pathway from *E. coli

The first committed step in fatty acid biosynthesis in *E. coli* is the conversion of acetyl-CoA to malonyl-CoA, catalyzed by the multicomponent acetyl-CoA carboxylase. In our previous study, when malonyl-CoA was directly supplied to the fatty acid synthase, we observed that a high initial malonyl-CoA concentration was inhibitory.⁷ We therefore sought to establish a more physiologically relevant *in vitro* system by including the acetyl-CoA carboxylase in the reaction mixture. To this end, we purified the four subunits of the *E. coli* carboxylase, AccA, *holo*-AccB (biotinylated AccB), AccC and AccD (Figure 3A). Because AccB must be post-translationally modified to be active,⁸ we purified it from an *E. coli* strain cultured with 15 μ M biotin and co-expressing AccB and BirA, the *E. coli* biotin-protein ligase.¹¹ By using a monomeric avidin column to remove traces of non-biotinylated AccB (*apo*-AccB), highly pure *holo*-protein was obtained, as verified by MALDI-TOF analysis.

Earlier studies had identified the optimal fatty acid synthase as a protein mixture consisting of 1 μ M FabA, FabB, FabD, FabF, FabG and FabH each, 10 μ M FabI and FabZ each, and 30 μ M *holo*-ACP and TesA each. To support *in situ* synthesis of malonyl-CoA, acetyl-CoA carboxylase was added to this optimized multi-enzyme system. Because the combined system required acetyl-CoA, bicarbonate, ATP, $MgCl_2$ and NADPH to produce fatty acyl-ACP, the optimal concentration of acetyl-CoA was determined by titrating this sole carbon source into a reaction mixture containing a high concentration of the carboxylase along with excess quantities of other substrates and cofactors (Figure 3B). The reaction velocity peaked at 600 μ M acetyl-CoA, which is approximately the intracellular concentration of acetyl-CoA in exponentially growing *E. coli*.¹² Excess acetyl-CoA was weakly inhibitory. We therefore fixed the acetyl-CoA concentration at 600 μ M. Because the peak reaction rate is sensitive to changing acetyl-CoA concentrations, care was taken to estimate velocity from the linear portion of each progress curve. The concentrations of ATP and NADPH were selected such that acetyl-CoA was the limiting substrate (assuming that palmitic acid was a representative product). To ensure that bicarbonate was not limiting, its concentration was fixed at 15 mM. Based on known K_{M,HCO_3^-} values of acetyl-CoA carboxylases from other species,^{13, 14} this value is likely to be ten-fold higher than the K_{M,HCO_3^-} of the *E. coli* enzyme. At a concentration of 15 mM, bicarbonate did not disrupt the pH of the reaction mixture. Moreover, changing the bicarbonate concentration to 10 mM or 20 mM did not change the enzyme activity significantly (data not shown). Care was taken while handling bicarbonate, including minimizing headspace in bicarbonate storage and reaction vials and adding bicarbonate last to a well-mixed reaction.

To quantify the acetyl-CoA carboxylase activity required for sustaining turnover of the fatty acid synthase at a maximal rate, we titrated the carboxylase keeping its subunits at an equimolar ratio (Figure 3C). The rate of fatty acid synthesis increased steadily until the carboxylase concentration was at least 20 times higher than the concentration of the ketosynthases. The maximum velocity observed, corresponding to a turnover rate of $0.5\ s^{-1}$,

was comparable to the rate of fatty acid synthesis under conditions where non-limiting concentrations of malonyl-CoA were supplied.

To ascertain the effects of individual subunits of the acetyl-CoA carboxylase on the overall rate of fatty acid synthesis, the concentrations of *holo*-AccB and AccC were individually varied, while maintaining the concentrations of the other subunits at 10 μ M (Figure 4). Because previous studies have shown that an active carboxyltransferase required an equimolar ratio of AccA and AccD,¹⁵ these two subunits were titrated together as an AccAD complex. Beyond ca. 1 μ M (i.e. the concentration of the individual ketosynthases in the reaction mixture), the concentrations of AccAD or AccC did not have a significant effect on the reaction rate. In contrast, *holo*-AccB positively influenced the overall rate with an apparent K_M of 18 μ M. In separate experiments, it was verified that removal of the hexa-His tag from this protein cofactor had no effect on its apparent K_M (J. Kuo, unpublished results). From all of the above results we concluded that, under conditions where the optimal fatty acid synthase comprised of 1 μ M FabA, FabB, FabD, FabF, FabG and FabH each, 10 μ M FabI and FabZ each, and 30 μ M *holo*-ACP and TesA each, the optimal concentrations of the acetyl-CoA carboxylase subunits were 10 μ M AccA, AccC and AccD each, and 30 μ M *holo*-AccB.

As a final validation of the robustness of this reconstituted biosynthetic pathway, three additional properties were verified. First, it was shown that the turnover rate of the *in vitro* system was proportional to its total protein content (Figure 5A). Second, under optimal turnover conditions, steady state was observed for ca. 10 turnovers of the complete system (normalized to the ACP concentration). For example, in the reaction shown in Figure 5B, the protein concentrations were as follows: 2 μ M AccA, AccC, AccD each, 0.2 μ M FabA, FabB, FabD, FabF, FabG and FabH each, 2 μ M FabI and FabZ each, and 6 μ M *holo*-AccB, *holo*-ACP and TesA. Over a time course of 5 min, a linear increase in product formation was observed up to a concentration of ca. 55 μ M palmitic acid equivalents, implying conversion of more than 50% of the acetyl-CoA substrate into product. Last but not least, we verified the fact that the turnover rate of the reconstituted system was saturated with respect to each protein component. As shown in Figure 5C, doubling the concentration of none of the components resulted in a significant rate enhancement of the multi-enzyme system.

***In vitro* product analysis**

The product profile of our complete reconstituted system was analyzed by silyl ester derivatization, followed by GC-MS. Under conditions of optimal turnover, the reaction was allowed to go to completion, and silyl ester derivatives of the following acids were identified: tetradecanoic acid, hexadecanoic acid, octadecanoic acid, *cis*-9-tetradecenoic acid, *cis*-9-hexadecenoic acid, and *cis*-11-octadecenoic acid (Figure 6A, trace 1). Among these different product species, C₁₆ and C₁₈ saturated and monounsaturated fatty acid were the most abundant. The position of double bond was conserved among different monounsaturated fatty acid species, presumably due to the high substrate specificity of the FabA isomerase for *trans*-2-decenoyl-ACP.¹⁶

Analysis of the factors responsible for unsaturated fatty acid production

The degree of unsaturation is an important characteristic of the product mixture obtained from fatty acid biosynthesis, both in physiology and in industry. It can, in principle, be influenced by several components of the system including the enoyl reductase (FabI), the two dehydratases (FabA and FabZ), and the two elongation ketosynthases (FabB and FabF) (Figure 1D). In *E. coli*, the biosynthetic intermediate *trans*-2-decenoyl-ACP lies at the branch point between saturated and monounsaturated fatty acids. In addition to its dehydratase activity, FabA catalyzes the reversible isomerization of *trans*-2-decenoyl-ACP

to *cis*-3-decenoyl-ACP, the only differentiating step leading to *cis*-unsaturated fatty acid biosynthesis.^{17, 18}

Using the optimal reconstituted system described above as a reference, we first investigated the effects of individual subunits on the ratio of unsaturated to saturated fatty acid product. As expected, in the absence of FabA, only trace quantities of unsaturated fatty acids were detected (Figure 6A, trace 2), although the turnover rate of the overall pathway was virtually unaffected (Figure 6B). In contrast, when FabZ was omitted, the rate of fatty acid synthesis was sharply reduced, and was partially restored when the concentration of FabA was increased to 10 μ M to compensate for the absence of FabZ (Figure 6B). Together, these findings are consistent with previous *in vivo* studies establishing that *fabZ* is an essential gene in *E. coli*¹⁹ and that FabA is not rate limiting in unsaturated fatty acid biosynthesis.²⁰ Unexpectedly however, the relative abundance of unsaturated fatty acids decreased when FabZ was omitted and FabA was increased (Figure 6A, trace 3). Moreover, simultaneously increasing the concentrations of both FabA and FabZ to 10 μ M did not increase the degree of unsaturation relative to the reference system harboring 1 μ M FabA and 10 μ M FabZ (Figure 6A, trace 4), nor did it enhance the turnover rate (Figure 6B).

Given our inability to alter metabolic flux distribution by manipulating the catalysts responsible for the branch-point reactions (i.e., FabA and FabZ), we sought to analyze the effects of downstream enzymes on the degree of unsaturation of the product. In particular, the ketosynthase catalyzes further elongation of the *cis*-3-decenoyl-ACP intermediate, thereby trapping the *cis*-olefin,²¹ whereas FabI catalyzes hydrogenation of the *trans*-2-decenoyl-ACP intermediate and thus commits the chain towards a fully saturated product.²² Although two ketosynthases (FabB and FabF) exist in *E. coli*, we have previously observed that increasing the concentration of FabF, but not FabB, inhibits the fatty acid synthase.⁷ Given that both FabB and FabF can elongate unsaturated as well as saturated fatty acids in the C₁₂ – C₁₆ range of chain lengths,²³ FabB was used to investigate the effect of chain elongation on the degree of unsaturation. Specifically, when the concentration of FabB was increased to 10 μ M, a significantly higher ratio of unsaturated fatty acids was observed (Figure 6A, trace 5) without altering the overall turnover rate of the system (Figure 6B). In contrast, when the concentration of FabI was reduced from 10 μ M to 1 μ M, the degree of unsaturation remained unchanged (Figure 6A, trace 6), and a drop in turnover rate was observed (Figure 6B).

A major advantage of a reconstituted *in vitro* system is the ability to quantify multifactorial effects such as the one described above. We therefore sought to systematically vary the relative and absolute concentrations of FabA and FabB with the goal of identifying conditions under which unsaturated fatty acid formation could be maximized without compromising the turnover rate of the metabolic pathway. For this, a quantitative GC-FID analytical procedure was implemented and performed simultaneously with steady state kinetic measurements. As shown in Figure 7, relative to optimal turnover conditions (where the FabB:FabA ratio is 1:1), the relative abundance of monounsaturated fatty acids decreases as FabA is increased, and increases as FabB is increased. The overall turnover rate is adversely affected as the concentration of either subunit becomes excessive relative to the other protein components of the fatty acid synthase. Under no conditions tested could the cumulative monounsaturated fatty acids exceed one-half of the overall products. Indeed, this threshold could not even be exceeded by a reduction of FabZ or FabI concentrations (data not shown). In all cases, the predominant monounsaturated fatty acids were *cis*-9-hexadecenoic acid, *cis*-11-octadecenoic acid (Figure 8); their ratio was not substantially influenced as the concentration of FabB increased.

Discussion

For at least two reasons, fatty acid biosynthesis in *E. coli* represents an ideal metabolic pathway to study the interplay between proteins, substrates and cofactors in intermediary metabolism. First, all of its products are derived from a single substrate, acetyl-CoA, and all the requisite reducing equivalents in this process are derived from NAD(P)H. Therefore, this biosynthetic pathway is particularly well suited to interrogating the factors that influence metabolic flux control. Second, even though none of the protein components in the pathway associate tightly, all intermediates in fatty acid biosynthesis remain protein-bound. Thus, it is likely that weak but specific protein-protein interactions are important for the channeling of reactive intermediates from one active site to the next. Elucidating the mechanistic principles underlying these phenomena in the context of fatty acid biosynthesis will likely have broader implications for other metabolic processes involving sequestered intermediates, such as polyketide biosynthesis.

Over the past decades, genetic, physiological, enzymological, and structural approaches have contributed to a wealth of knowledge regarding this central metabolic process.^{17, 24–27} Notwithstanding these advances, quantitative description of fatty acid metabolism requires the ability to manipulate the properties and concentrations of individual proteins, substrates and cofactors with precision. We have therefore reconstituted *in vitro* the entire biosynthetic pathway from *E. coli* that converts acetyl-CoA to free fatty acids. By the addition of the four-component acetyl-CoA carboxylase to the previously reconstituted ten-component fatty acid synthase,³ and by titrating each protein individually, a maximum turnover rate of 0.5 s⁻¹ was achieved through at least ten turnovers. This turnover rate is comparable to previous reported estimated k_{cat} value for FAS activity in *E. coli*.⁷ Furthermore, stoichiometric conversion of NADPH into product enabled the development of a facile UV spectrophotometric assay for the entire metabolic pathway. In addition to the acetyl-CoA carboxylase, FabZ and FabI were found to be rate limiting, and therefore were required at higher concentrations relative to the other subunits in order to attain maximum turnover rates. Consistent with *in vivo* analysis,¹ the predominant products were C₁₆ and C₁₈ saturated and monounsaturated fatty acids. Thus, our reconstituted system mimics fatty acid biosynthesis under physiological conditions.

To highlight the utility of this reconstituted system, we investigated the quantitative relationships between individual protein concentrations and the degree of unsaturation of the fatty acid product mixture. Extensive genetic analysis has highlighted the physiological relevance of this parameter in *E. coli*.^{3, 28} In addition, the relative abundance of unsaturated fatty acids is an important determinant of biodiesel quality.^{4, 5} FabA and FabB were identified as the key elements that control the metabolic flux distribution between monounsaturated and saturated fatty acid products. Furthermore, our experiments demonstrated that this ratio could be systematically varied between 10–50% without sacrificing the turnover efficiency of this metabolic pathway. By reducing the ratio of FabB:FabA, the degree of unsaturation could be decreased; conversely, by increasing this enzyme ratio, a more unsaturated product could be obtained. Given that FabA is the first enzyme in the metabolic branch leading to monounsaturated fatty acids, this result is somewhat counterintuitive. It can, however, be rationalized as follows. We speculate that a relatively small amount of FabA is sufficient to bring *trans*-2-decenoyl-ACP and *cis*-3-decenoyl-ACP into equilibrium with each other, at which point the carbon flux toward monounsaturated fatty acid attains a maximum value. Moreover, whereas the external equilibrium results in comparable amounts of the two isomers in the absence of downstream reactions,²⁹ FabA has a high affinity for *cis*-3-decenoyl-ACP, and can therefore sequester this intermediate at high concentrations. Further biochemical and mutagenesis studies are warranted to test this hypothesis.

Supplementary Material

Refer to Web version on PubMed Central for supplementary material.

Acknowledgments

We thank Haibo Wang and Stephen del Cardayre at LS9, Inc., for access to their GC-MS/GC-FID facility, and for insightful discussions. We would also like to thank Shripa Patel of Stanford Protein and Nucleic Acid Facility for the help with MALDI-TOF analyses.

Abbreviations

ACC	acetyl-CoA carboxylase
ACP	acyl carrier protein
BSTFA	bistrifluoroacetamide
GC-FID	gas chromatography-flame ionization detector
GC-MS	gas chromatography-mass spectrometry
TE	thioesterase
TMCS	trimethylchlorosilane

References

1. Liu T, Vora H, Khosla C. Quantitative analysis and engineering of fatty acid biosynthesis in *E. coli*. *Metab Eng.* 2010; 12:378–386. [PubMed: 20184964]
2. Neidhardt, FC.; Curtiss, R. *Escherichia coli* and *Salmonella* cellular and molecular biology, 2nd ed. ASM Press; Washington, D.C: 1999. p. 1CD-ROM (4 3/4 in.) +
3. Mansilla MC, Cybulski LE, Albanesi D, de Mendoza D. Control of membrane lipid fluidity by molecular thermosensors. *J Bacteriol.* 2004; 186:6681–6688. [PubMed: 15466018]
4. Tyson, KS.; McCormick, RL. United States. Dept. of Energy. Office of Energy Efficiency and Renewable Energy., and National Renewable Energy Laboratory (U.S.). Nrel/Tp 540-40555. 3. National Renewable Energy Laboratory; Golden, CO: 2006. Biodiesel handling and use guidelines; p. ivp. 61
5. Ramos MJ, Fernandez CM, Casas A, Rodriguez L, Perez A. Influence of fatty acid composition of raw materials on biodiesel properties. *Bioresour Technol.* 2009; 100:261–268. [PubMed: 18693011]
6. Yu X, Khosla Chaitan. Engineering *Escherichia coli* for Biotransformation of Biomass into Fatty Acid Derived Fuels. *Current chemical biology.* 2012; 6:7–13.
7. Yu X, Liu T, Zhu F, Khosla C. In vitro reconstitution and steady-state analysis of the fatty acid synthase from *Escherichia coli*. *Proc Natl Acad Sci U S A.* 2011; 108:18643–18648. [PubMed: 22042840]
8. Chapman-Smith A, Turner DL, Cronan JE Jr, Morris TW, Wallace JC. Expression, biotinylation and purification of a biotin-domain peptide from the biotin carboxy carrier protein of *Escherichia coli* acetyl-CoA carboxylase. *Biochem J.* 1994; 302(Pt 3):881–887. [PubMed: 7945216]
9. Fall RR, Vagelos PR. Acetyl coenzyme A carboxylase. Molecular forms and subunit composition of biotin carboxyl carrier protein. *J Biol Chem.* 1972; 247:8005–8015. [PubMed: 4565671]
10. Nenortas E, Beckett D. Purification and characterization of intact and truncated forms of the *Escherichia coli* biotin carboxyl carrier subunit of acetyl-CoA carboxylase. *J Biol Chem.* 1996; 271:7559–7567. [PubMed: 8631788]
11. Streaker ED, Beckett D. The biotin regulatory system: kinetic control of a transcriptional switch. *Biochemistry.* 2006; 45:6417–6425. [PubMed: 16700552]

12. Bennett BD, Kimball EH, Gao M, Osterhout R, Van Dien SJ, Rabinowitz JD. Absolute metabolite concentrations and implied enzyme active site occupancy in *Escherichia coli*. *Nat Chem Biol*. 2009; 5:593–599. [PubMed: 19561621]
13. Hugler M, Krieger RS, Jahn M, Fuchs G. Characterization of acetyl-CoA/propionyl-CoA carboxylase in *Metallosphaera sedula*. Carboxylating enzyme in the 3-hydroxypropionate cycle for autotrophic carbon fixation. *Eur J Biochem*. 2003; 270:736–744. [PubMed: 12581213]
14. Livne A. Acetyl-coenzyme A carboxylase from the marine prymnesiophyte *Isochrysis galbana*. *Plant & Cell Physiology*. 1990; 31:851.
15. Choi-Rhee E, Cronan JE. The biotin carboxylase-biotin carboxyl carrier protein complex of *Escherichia coli* acetyl-CoA carboxylase. *J Biol Chem*. 2003; 278:30806–30812. [PubMed: 12794081]
16. Heath RJ, Rock CO. Regulation of fatty acid elongation and initiation by acyl-acyl carrier protein in *Escherichia coli*. *J Biol Chem*. 1996; 271:1833–1836. [PubMed: 8567624]
17. White SW, Zheng J, Zhang YM, Rock. The structural biology of type II fatty acid biosynthesis. *Annu Rev Biochem*. 2005; 74:791–831. [PubMed: 15952903]
18. Leesong M, Henderson BS, Gillig JR, Schwab JM, Smith JL. Structure of a dehydratase-isomerase from the bacterial pathway for biosynthesis of unsaturated fatty acids: two catalytic activities in one active site. *Structure*. 1996; 4:253–264. [PubMed: 8805534]
19. Liang R, Liu J. In-frame deletion of *Escherichia coli* essential genes in complex regulon. *Biotechniques*. 2008; 44:209–210. 212–205. [PubMed: 18330348]
20. Clark DP, DeMendoza D, Polacco ML, Cronan JE Jr. Beta-hydroxydecanoyl thio ester dehydrase does not catalyze a rate-limiting step in *Escherichia coli* unsaturated fatty acid synthesis. *Biochemistry*. 1983; 22:5897–5902. [PubMed: 6362720]
21. Feng Y, Cronan JE. *Escherichia coli* unsaturated fatty acid synthesis: complex transcription of the *fabA* gene and in vivo identification of the essential reaction catalyzed by *FabB*. *J Biol Chem*. 2009; 284:29526–29535. [PubMed: 19679654]
22. Heath RJ, Rock CO. Enoyl-acyl carrier protein reductase (*fabI*) plays a determinant role in completing cycles of fatty acid elongation in *Escherichia coli*. *J Biol Chem*. 1995; 270:26538–26542. [PubMed: 7592873]
23. Garwin JL, Klages AL, Cronan JE Jr. Structural, enzymatic, and genetic studies of beta-ketoacyl-acyl carrier protein synthases I and II of *Escherichia coli*. *J Biol Chem*. 1980; 255:11949–11956. [PubMed: 7002930]
24. Magnuson K, Jackowski S, Rock CO, Cronan JE Jr. Regulation of fatty acid biosynthesis in *Escherichia coli*. *Microbiol Rev*. 1993; 57:522–542. [PubMed: 8246839]
25. Campbell JW, Cronan JE Jr. Bacterial fatty acid biosynthesis: targets for antibacterial drug discovery. *Annu Rev Microbiol*. 2001; 55:305–332. [PubMed: 11544358]
26. Raetz CR. Molecular genetics of membrane phospholipid synthesis. *Annu Rev Genet*. 1986; 20:253–295. [PubMed: 3545060]
27. Hopwood DA, Sherman DH. Molecular genetics of polyketides and its comparison to fatty acid biosynthesis. *Annu Rev Genet*. 1990; 24:37–66. [PubMed: 2088174]
28. Pradenas GA, Paillavil BA, Reyes-Cerpa S, Perez-Donoso JM, Vasquez CC. Reduction of the monounsaturated fatty acid content of *Escherichia coli* results in increased resistance to oxidative damage. *Microbiology*. 2012; 158:1279–1283. [PubMed: 22343353]
29. Guerra DJ, Browse JA. *Escherichia coli* beta-hydroxydecanoyl thioester dehydrase reacts with native C10 acyl-acyl-carrier proteins of plant and bacterial origin. *Arch Biochem Biophys*. 1990; 280:336–345. [PubMed: 2195995]

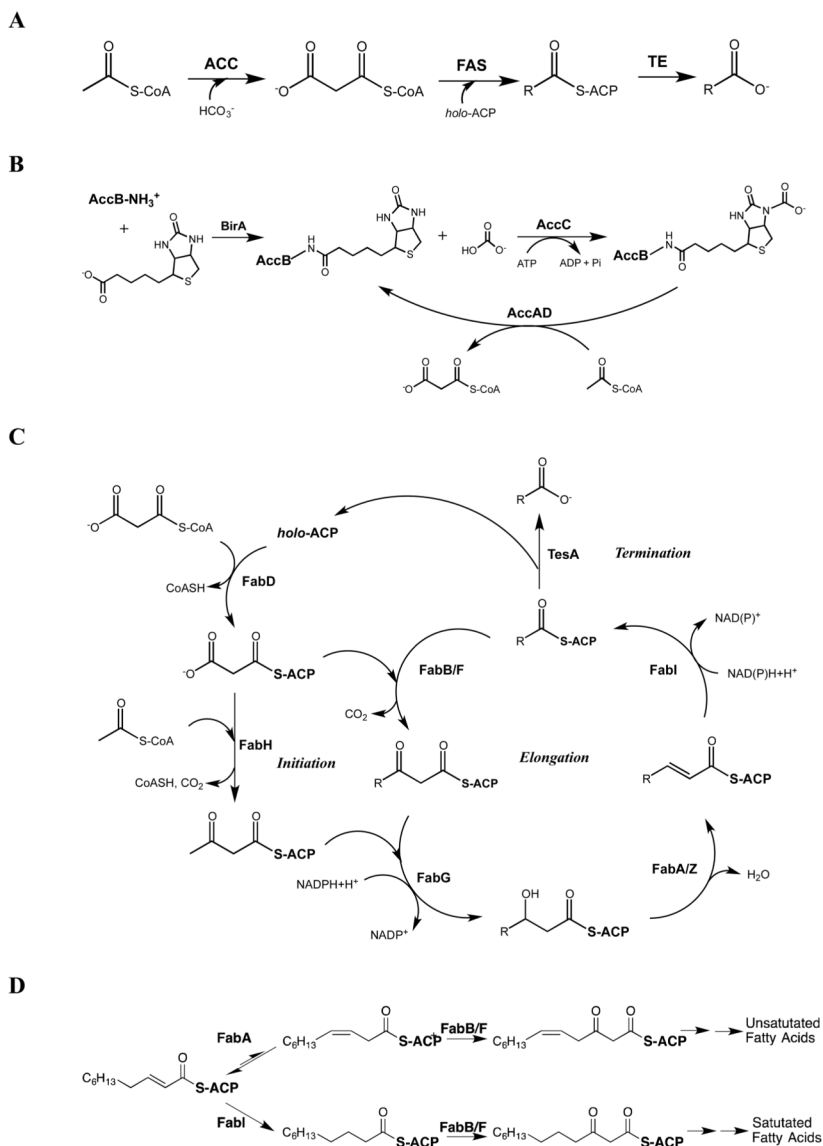


Figure 1. The biosynthetic pathway of fatty acids and derivatives in *E. coli*

(A) The overall reaction scheme involving the acetyl-CoA carboxylase (ACC), the fatty acid synthase (FAS) and the thioesterase (TE). (B) Biotinylation of the biotin carboxyl carrier protein (AccB) is catalyzed by BirA. The resulting *holo*-AccB participates in ACC-catalyzed carboxylation of acetyl-CoA. (C) Production of saturated fatty acids from acetyl-CoA and malonyl-CoA, catalyzed by the 9-component FAS (FabA, FabB, FabD, FabF, FabG, FabH, FabI, FabZ, ACP) and the TE (TesA). (D) Unsaturated fatty acids are synthesized via the isomerization of a common intermediate, *trans*-2-decenoyl-ACP, in a reaction catalyzed by FabA, a dual-function isomerase and dehydratase. Subsequent elongation of the *cis*-3-decenoyl-ACP product traps the *cis*-olefin, leading to eventual release of monounsaturated fatty acids.

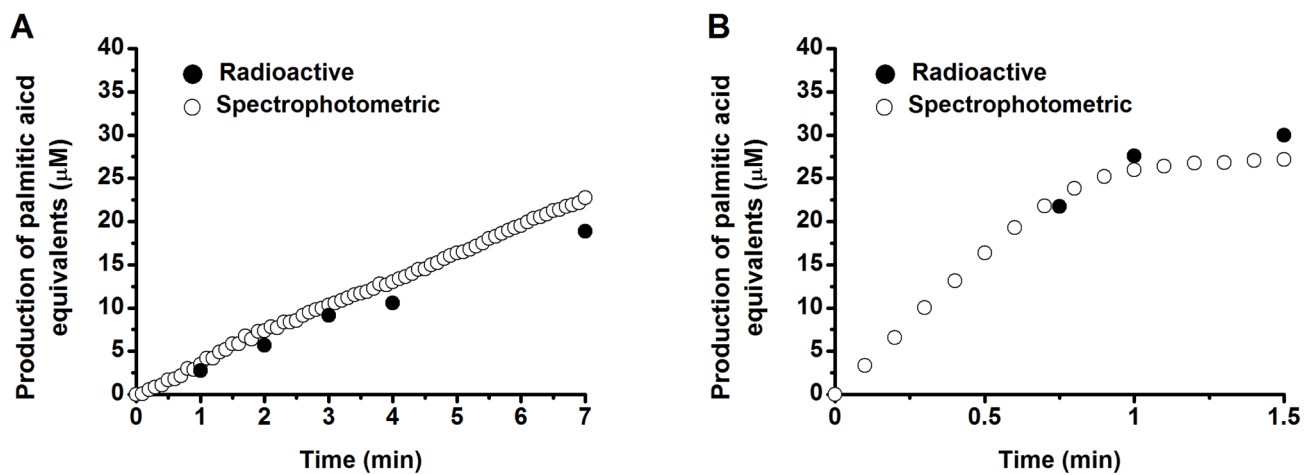


Figure 2. Comparison of radioactive and spectrophotometric assays in measuring activities of reconstituted fatty acid synthases

(A) Reference FAS, consisting of $1\ \mu\text{M}$ FabABDFGHIZ, $10\ \mu\text{M}$ *holo*-ACP, and $10\ \mu\text{M}$ TesA. (B) Optimized FAS, consisting of $1\ \mu\text{M}$ FabABDFGH, $10\ \mu\text{M}$ FabIZ, $30\ \mu\text{M}$ *holo*-ACP, and $30\ \mu\text{M}$ TesA. Reaction conditions were otherwise identical: $100\ \mu\text{M}$ acetyl-CoA, $500\ \mu\text{M}$ malonyl-CoA, and $1.3\ \text{mM}$ NADPH. Under optimal conditions, the initial rate of fatty acid production was missed when a radioactive assay was used. See also Table 1 for a comparison of the measured rate constants.

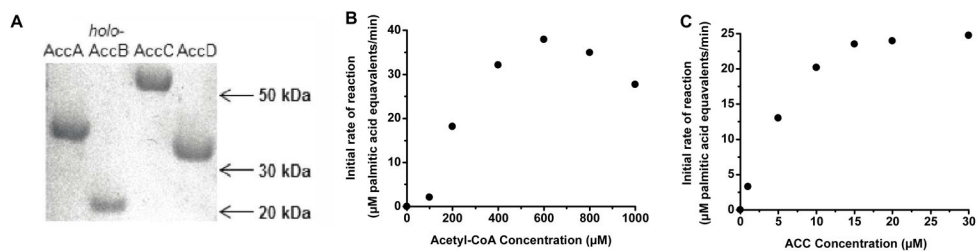


Figure 3. Reconstitution of acetyl-CoA carboxylase

(A) SDS-PAGE analysis of the acetyl-CoA carboxylase subunits. AccA, *holo*-AccB, AccC and AccD. AccB migrates around 20 kDa in a Tris-glycine SDS-PAGE system, because of its long Pro- and Ala-rich segment between residues 34 and 101⁷. (B) Effect of acetyl-CoA concentration on the initial reaction velocity of the complete reconstituted system shown in Figure 1. Reaction condition: 30 μM AccABCD, 1 μM FabABDFGH, 10 μM FabIZ, 30 μM *holo*-ACP, 30 μM TesA, 15 mM bicarbonate, 1 mM ATP, 5 mM MgCl_2 , and 1.3 mM NADPH. (C) Dependence of overall turnover rate on acetyl-CoA carboxylase concentration in the complete reconstituted system. Reactions contain varying concentrations of the carboxylase complex, 1 μM FabABDFGH, 10 μM FabIZ, 30 μM *holo*-ACP, 30 μM TesA (TE), 600 μM acetyl-CoA, 15 mM sodium bicarbonate, 1 mM ATP, 5 mM MgCl_2 , and 1.3 mM NADPH.

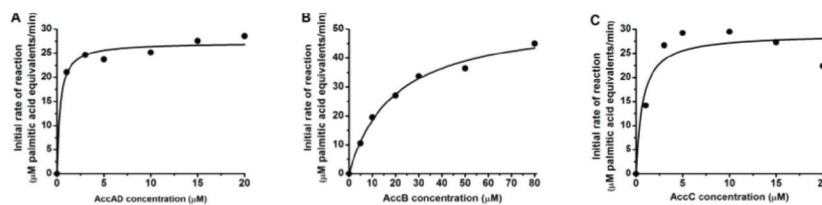


Figure 4. Effect of ACC activity on the initial reaction velocity of the complete reconstituted system shown in Figure 1

(A) Titration of AccAD complex. (B) Titration of AccB subunit. (C) Titration of AccC subunit. Reactions contain varying concentrations of ACC subunits or complex in question, 1 μM FabABDFGH, 10 μM FabIZ, 30 μM *holo*-ACP, 30 μM TesA (TE), 600 μM acetyl-CoA, 15 mM sodium bicarbonate, 1 mM ATP, 5 mM MgCl_2 , and 1.3 mM NADPH.

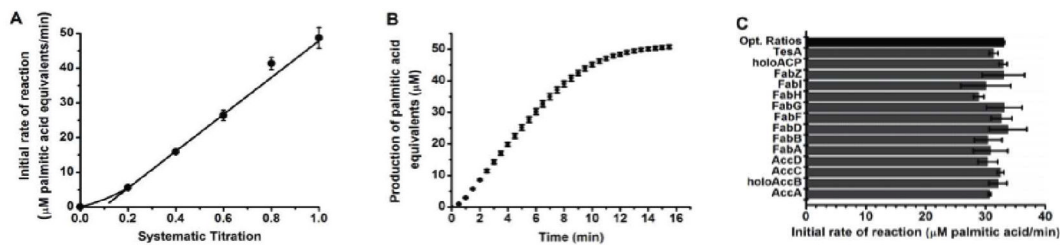


Figure 5. Kinetic properties of overall reconstituted pathway shown in Figure 1

(A) Kinetic linearity of overall reconstituted pathway. Reaction conditions: 2–10 μM AccAD, AccC, 6–30 μM *holo*-AccB, 0.2–1 μM FabABDFGH, 2–10 μM FabIZ, 6–30 μM *holo*-ACP, 6–30 μM TesA, 600 μM acetyl-CoA, 15 mM bicarbonate, 1 mM ATP, 5 mM MgCl_2 , and 1.3 mM NADPH. (B) Palmitic acid product formation in 5-fold dilution system. (C) Initial reaction rates of optimized reconstituted systems with an individual enzyme concentration doubled. Experiments were performed in two-fold dilution system.

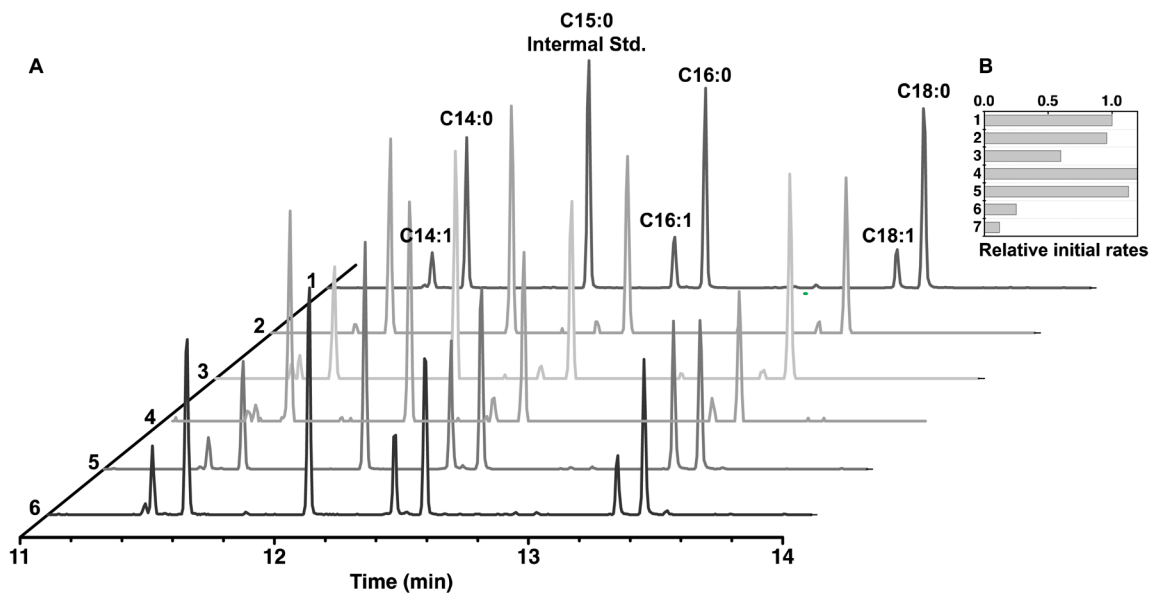


Figure 6. GC-MS and kinetic analysis of factors responsible for unsaturated fatty acid production

(A) Individual GC-MS traces correspond to the following experiments: (1) optimized system (2); optimized system without FabA; (3) optimized system without FabZ but with 10 μM FabA; (4) optimized system with 10 μM each of FabA and FabZ; (5) optimized system with 10 μM FabB; and (6) optimized system with 1 μM FabI. Labeled peaks correspond to BSTFA derivatized fatty acids produced by TesA-catalyzed hydrolysis. All other unlabeled peaks are impurities most likely derived from the plastics involved in the product extraction and storage process. (B) Relative rates of fatty acid biosynthesis under the different conditions described in part A. The graph also includes data for the synthase lacking FabZ (bar 7), which has a low but measurable turnover rate.

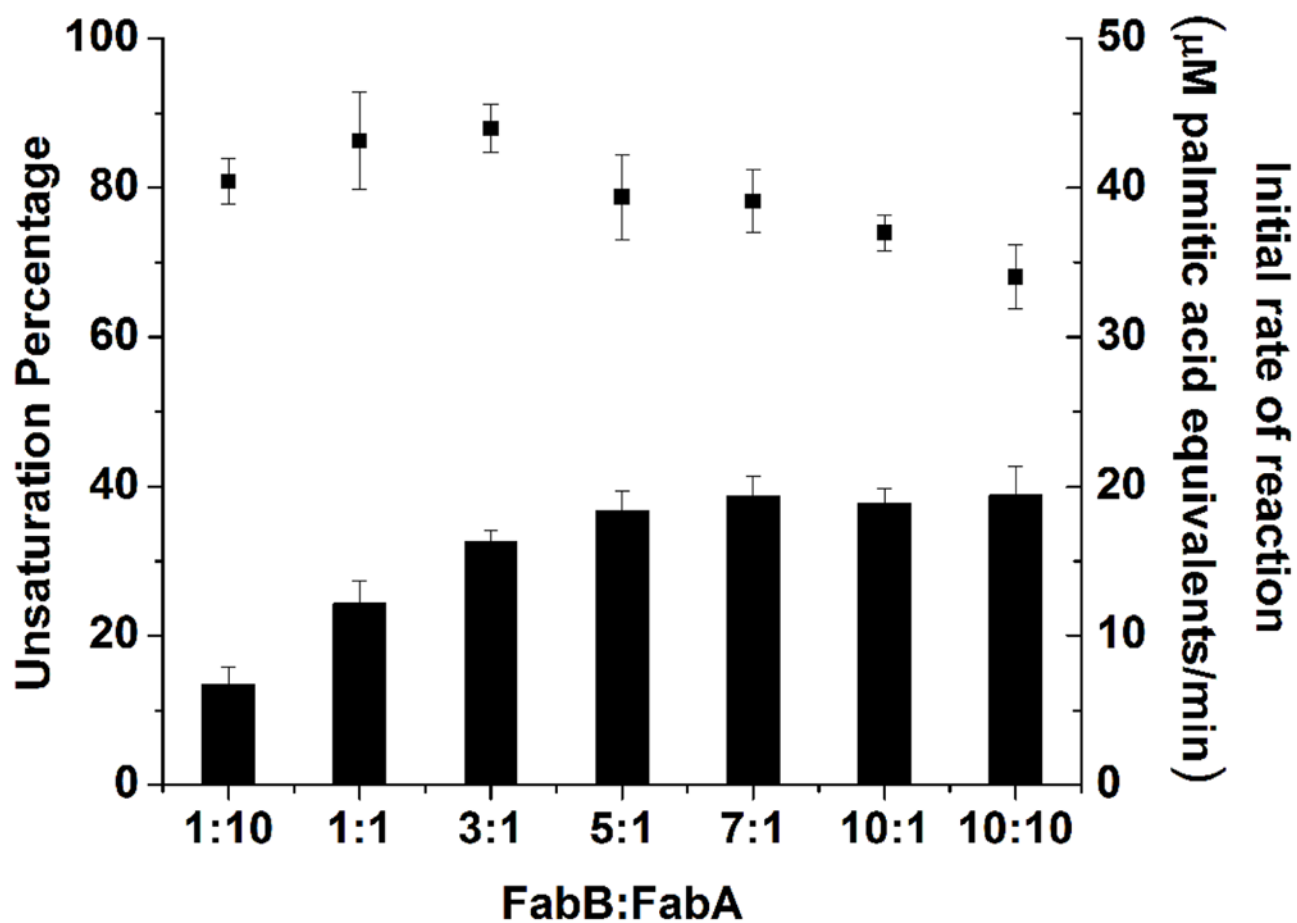


Figure 7. Quantitative analysis of the effect of FabB:FabA ratio on unsaturated fatty acid production

The bars correspond to the relative abundance of unsaturated fatty acid in the product mixture (left y-axis), and the black squares represent the initial turnover rate of the overall pathway (right y-axis). All data are means \pm s.d. (n=3). For experimental details, see text.

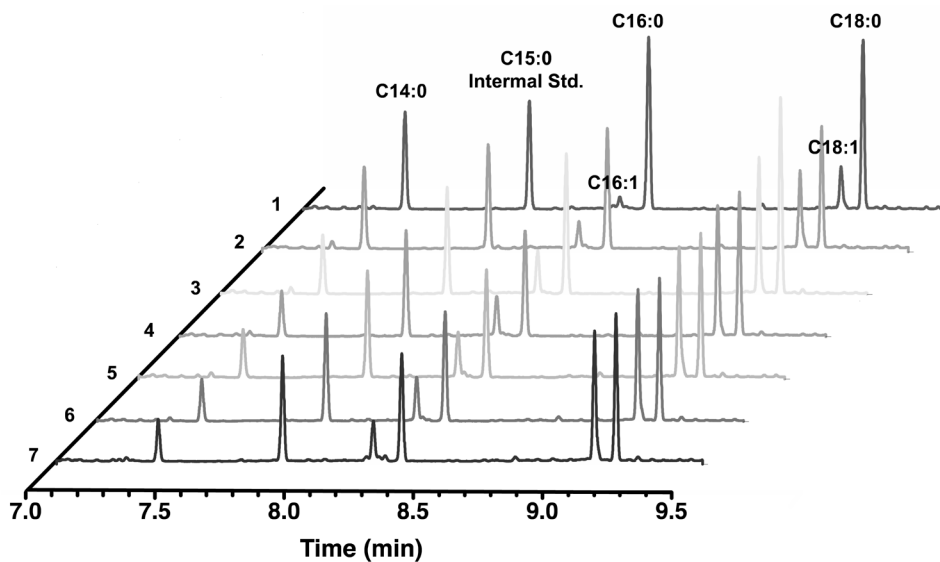


Figure 8. GC-FID chromatographic analysis of product profiles under varying FabB:FabA ratios

The relevant assay conditions are: (1) 1 μ M FabB, 10 μ M FabA; (2) 1 μ M FabB, 1 μ M FabA; (3) 3 μ M FabB, 1 μ M FabA; (4) 5 μ M FabB, 1 μ M FabA; (5) 7 μ M FabB, 1 μ M FabA; (6) 10 μ M FabB, 1 μ M FabA; and (7) 10 μ M FabB, 10 μ M FabA. Chromatographic peaks were identified through comparison of retention time with authentic standards.

Table 1

Comparison of the initial rates of reaction measured by radioactive and spectrophotometric assays. Conditions in reference system were derived as described previously.⁷ For details, see Figure 2.

Initial rate of reaction (μM palmitic acid equivalents/min)	Reference	Optimized
Radioactive assay	3.0	>23.5
Spectrophotometric assay	3.7	35.2